

# Numerical investigation of natural convection of cavity receiver for low power application

L. C. Ngo<sup>1</sup>, T. Bello-Ochende<sup>2</sup> and J. P. Meyer<sup>1</sup>

1 Department of Mechanical and Aeronautical Engineering, University of Pretoria, Pretoria, Private Bag X20, Hatfield 0028, South Africa

2 Department of Mechanical Engineering, University of Cape Town, Private Bag X3, Rondebosch 7701, Cape Town, South Africa

## ABSTRACT

A parabolic dish/cavity receiver configuration is one of the solar thermal systems used for light-heat conversion at high temperature. Such systems are subject to continuous changes in ambient conditions such as wind, solar insolation and ambient temperature. These environmental variations, as well as changes in receiver inclination angle, affect the overall receiver performance leading to energy loss. Natural convection contributes a significant fraction of the energy loss and hence a thorough understanding of its characteristics is essential to effectively minimise it in order to improve the system efficiency. A three-dimensional numerical investigation was conducted on a modified cavity receiver to quantify the convective components of the total heat loss and to determine the effects of the operating temperature, receiver inclination angle and aperture size on the heat loss. The effects of the variation of air properties were accounted for by using polynomial relationships for density, specific heat capacity at constant pressure, dynamic viscosity and thermal conductivity in the simulation. The calculated natural convection heat loss showed a non-linear dependence on the inclination angle and aperture size. Visualisation results such as temperature contours were also presented to gain an insight into the effects of natural convection.

**Keywords:** Parabolic dish; Cavity receiver; Natural convection; Nusselt number

## 1. INTRODUCTION

The conversion of solar energy into electricity has been receiving more and more attention in recent years. Sunlight is the world's largest energy source and the amount that can be readily accessed with existing technology greatly exceeds the world's primary energy consumption. Furthermore, sunlight is free, clean, renewable and technically exploitable in most parts of the inhabited earth.

Parabolic dish/cavity receiver configurations are some of the solar thermal systems used for light-heat conversion at high temperature. Such systems are subject to continuous changes in ambient conditions such as wind, solar insolation and ambient temperature. These environmental variations, as well as changes in receiver inclination angle, affect the overall receiver performance leading to energy loss.

The total energy loss of solar receivers, which includes convection and radiation heat loss to the air and conduction heat loss through the insulation, plays a dominant role in the light-heat conversion. The radiation heat loss is dependent on the cavity wall temperature, the shape factors and emissivity/absorptivity of the receiver walls, while conduction heat loss is dependent on the receiver wall temperature and the insulation material.

Analytical methods for predicting the radiative and conductive heat losses from a cavity receiver are fairly straightforward. However, this is not the case for convective heat loss analysis. The complexity of geometry, temperature and velocity fields in and around the receiver makes it difficult to use existing analytical models for predicting convective heat loss.

In the literature, there are a number of papers concerning natural convection heat transfer in open cavities. For instance, LeQuere et al. (1981) investigated heat loss characteristics of two different-sized cubical cavities. They considered variations in receiver operating temperature and angle in their study. They found convection heat loss to be strongly dependent on the cavity inclination. Harris and Lenz (1985) presented a study conducted by Koenig and Marvin that empirically derived a correlation for convective heat loss from cylindrical cavity-type receivers, including the effects of variation in operating temperature and angle. An analytical model for convective heat loss for an open cubical cavity receiver was presented by Clausing (1983). The Clausing model was developed for a central receiver operating at much higher temperatures.

Siangsukone and Lovegrove (2002) presented work on modelling and simulation of the Australia National University (ANU) 400m<sup>2</sup> paraboloidal dish concentrator system with a direct steam-generating cavity receiver and the steam line. Taumoefolau and Lovegrove (2002) presented an experimental investigation based on an isothermal electrically heated model cavity receiver. Sendhil Kumar and Reddy (2007) presented a two-dimensional model to

estimate natural convection heat loss from the modified cavity receiver of a fuzzy focal solar dish concentrator. Both insulation conditions and no insulation conditions were used for estimation of heat loss. The analysis of the receiver was carried out based on the assumption of the uniform and maximum solar flux distribution in the central plane of the receiver. Sendhil Kumar and Reddy (2008) presented a numerical investigation of natural convective heat loss from three types of receivers for a fuzzy focal solar dish concentrator, namely cavity receiver, semi-cavity receiver and modified cavity receiver. Reddy and Sendhil Kumar (2008) presented a numerical study of combined laminar natural convection and surface radiation heat transfer in a modified cavity receiver of solar parabolic dish collector. A comparison of two-dimensional and three-dimensional natural convection heat loss from a modified cavity receiver was carried out by Reddy and Sendhil Kumar (2009). Prakash et al. (2009) reported experimental and numerical studies of the steady-state convection heat losses occurring from a downward-facing cylindrical cavity receiver. From all the data points, Nusselt number correlations as a function of receiver aperture diameter were proposed for the natural convection heat losses. Wu et al. (2011) conducted a three-dimensional numerical study to investigate the influence of aperture characteristics, i.e. aperture position and size on natural convection heat loss of a heat-pipe receiver accounting for air property variation with temperature.

In this paper, a numerical investigation of a modified cavity receiver was conducted to quantify the natural convection heat loss, and to determine the effects of the operating temperature, receiver inclination angle and aperture size on the heat loss. Furthermore, visualisation results, such as temperature contours, were also presented to gain an insight into the effects of natural convection. The Boussinesq and non-Boussinesq fluid models were used in the numerical investigation and a comparison was made between them. For the fluids modelled as Boussinesq incompressible, the density was regarded as a constant property everywhere except in the body force terms of the momentum equations. In this approximation, the density was treated as a linear function of temperature only and was assumed to be independent of pressure.

The focus was on modified cavity receivers employed in medium and high-temperature solar dish systems with operating temperature up to 1 000 K and accounting for the air property variations. The Boussinesq approximation, which was applied in previous numerical investigations for modified cavity receivers (Sendhil Kumar and Reddy, 2007; Sendhil Kumar and Reddy, 2008; Reddy and Sendhil Kumar, 2008; Reddy and Sendhil Kumar, 2009), leads to considerable deviations at high operating temperatures, and can no longer be applicable to such receivers, because the air properties change significantly with the remarkable operating temperature increments. For example, when the air temperature rises from the ambient temperature of 300 K to the receiver's operating temperature of 1 000 K, air density decreases by 77.72%; thermal conductivity increases by 780.76%; kinematic viscosity increases by 252.95%,

and these significant changes in air physical properties definitely have a very important influence on natural convection heat loss.

## 2. PHYSICAL AND MATHEMATICAL MODEL

The modified cavity receiver without insulation suggested by Reddy and Sendhil Kumar (2007) is considered in the analysis. The collector system consists of a parabolic dish collector operating in tracking mode as shown in figure 1. The receiver is made of copper tubing with an opening aperture diameter ( $d$ ) and cavity diameter ( $D$ ) of 180 mm. The copper tubes are wound spirally to get the respective shape of receiver. The outer surface of the cavity receiver is completely covered with opaque insulation. Two assumptions are made for modelling the cavity receiver: (a) the surfaces of the tube are uniform and smooth; (b) the temperature of air flowing through the copper tube is the same as the surface temperature of the tube.

Natural convection heat loss is estimated at different inclination angles of the receiver from  $\varphi = 0$  (cavity receiver aperture facing sideways) to  $\varphi = 90^\circ$  (cavity aperture facing downwards). To investigate the effects of aperture diameter, the aperture diameter is varied from 60 mm to 120 mm.

For natural convection in the cavity receiver, the flow and heat transfer simulations are based on the simultaneous solution of equations describing the conservation of mass, momentum and energy of the system.

Continuity equation:

$$\Delta \cdot (\rho \mathbf{V}) = 0 \quad (1)$$

Momentum equation:

$$\rho \mathbf{V} \cdot \nabla (\rho \mathbf{V}) = \rho \mathbf{X} - \nabla p + \nabla^2 (\mu \mathbf{V}) \quad (2)$$

Energy equation:

$$\rho \mathbf{V} \cdot \nabla (\rho c_p T) = \nabla^2 (kT) \quad (3)$$

Where  $\rho$  is the density of air,  $\text{kg/m}^3$ ,  $\mathbf{V}$  is the velocity vector of air,  $\text{m/s}$ ,  $\mathbf{X}$  is the mass force vector,  $\text{N/kg}$ ,  $p$  is the pressure,  $\text{Pa}$ ,  $\mu$  is dynamic viscosity,  $\text{kg/(m.s)}$ ,  $c_p$  is the specific heat capacity at constant pressure,  $\text{J/(kg.K)}$ ,  $k$  is thermal conductivity of air,  $\text{W/(m.K)}$ , and  $T$  is temperature in Kelvin.

Polynomial relationships for density, specific heat capacity at constant pressure and dynamic viscosity are used to account for air property variation with temperature (Zografos et al., 1987).

$$\rho = 7.4992 \times 10^{-9} T^3 + 1.6487 \times 10^{-5} T^2 - 1.2366 \times 10^{-2} T + 3.6508 \quad (4)$$

$$c_p = 1.3864 \times 10^{-13} T^4 - 6.4747 \times 10^{-10} T^3 + 1.0234 \times 10^{-6} T^2 - 4.3282 \times 10^{-4} T + 1.0613 \quad (5)$$

$$\mu = 1.3864 \times 10^{-15} T^3 - 1.4346 \times 10^{-11} T^2 + 5.0523 \times 10^{-8} T + 4.1130 \times 10^{-6} \quad (6)$$

The convective heat transfer coefficient can be expressed as:

$$h_c = \frac{Nu k}{D} \quad (7)$$

where  $Nu$  is the Nusselt number and  $D$  is the receiver cavity diameter. The Nusselt numbers were calculated using STAR-CCM+ 7.06.

The convective heat loss from the modified cavity receiver is given as:

$$Q_c = h_c A (T_s - T_\infty) \quad (8)$$

### 3. NUMERICAL PROCEDURE AND VALIDATION

#### 3.1 Numerical procedure

A finite volume-based CFD code, STAR-CCM+ 7.06, was employed in the 3D simulation of the natural convection through the aperture of the cavity receiver. Figure 2 schematically represents the computational grid of the cavity receiver. In reality, the receiver was surrounded by an infinite atmosphere with a limiting temperature equal to ambient air temperature. In the numerical analysis, the region outside the cavity was represented by a spherical enclosure. The size of the enclosure was increased until it had an insignificant effect on fluid and heat flows in the vicinity of the receiver. It was found that in STARCCM+, the diameter of the spherical enclosure should be about 10 times the diameter of the receiver to achieve this.

A mesh refinement was performed on the cavity receiver, investigating the average Nusselt number on the hot inner surfaces of the cavity receiver ( $T_s = 800$  K and  $Ra = 10^6$ ). Table 1 presents the average Nusselt numbers obtained for five different grids at 90 degrees inclination angle of the receiver. The relative deviation for the Nusselt number

between grid 1 and 2 was less than 1%. Since the differences between the two were minor, we chose grid 2 for all the simulations presented in this work. This was considered as a good trade-off between accuracy and cost of time.

The cells were very small in the region inside the cavity and nearby the receiver but increased in size gradually towards the spherical enclosure wall. Prism layer cells were also used on the walls of the cavity receiver. This layer of cells was necessary to improve the accuracy of the flow solution. Since the Rayleigh numbers (Ra) encountered were less than  $10^8$ , the laminar, steady-state and three-dimensional governing equations were solved by STAR-CCM+ using an implicit solver.

### **3.1.1 Boundary conditions**

An isothermal boundary condition was applied to the internal receiver surfaces and the outer surface on the aperture plane as shown in Figure 3. The temperature was varied from 400-1 000 K. The outer spherical walls of the receiver were treated as adiabatic since it was covered with insulation to prevent heat loss.

The outer domain was treated as a pressure outlet boundary condition. The wall temperature of the entire spherical enclosure was set to an ambient temperature of 300 K.

### **3.2 Validation**

To validate the present numerical procedure of the modified cavity receiver, a typical case of 3-D laminar natural convection heat transfer from an isothermal horizontal open hemispherical cavity reported by Khubeiz et al. (2002) has been considered. The results of the theoretical analysis, numerical calculation and experimental procedure are presented in the Nusselt and Rayleigh number relations:  $Nu_D = 0.296Ra_D^{1/4}$ ,  $Nu_D = 0.340Ra_D^{1/4}$  and  $Nu_D = 0.316 Ra_D^{1/4}$  respectively. This present numerical procedure has been validated using glycerine as the working fluid. The isotherms of the upward facing hemispherical open cavity at Ra of  $1.1511 \times 10^7$  are shown in figure 4.

The area-weighted average Nusselt numbers for the hot surface of the hemisphere were obtained for two different Rayleigh numbers. The results are given in table 2. It was observed that the present numerical procedure was in good agreement with the experimental data with maximum deviation approximately 6.45%.

## 4. RESULTS AND DISCUSSION

### 4.1 Effects of receiver inclination angle and operating temperature on natural convection heat loss

To estimate the natural convection heat loss from the modified cavity receiver, the temperature was varied from 400 K to 1 000 K. Figure 5 shows the temperature contours of the modified cavity receiver on the symmetry plane operating at 400 K for different inclinations of the receiver.

The behaviour of air in the cavity receiver was completely different at varying inclination angles of the receiver. In the downwards-facing position of  $90^\circ$ , the cavity was almost dominated by the stagnant zone, thus convection heat loss out of the receiver was small. When the receiver inclination angle was varied anticlockwise, the stagnant zone decreased and this increased the convective zone where most of the heat transfer mainly happened. The near stagnant air and almost uniform temperature within the stagnation zone suggests that it does not take part in the convective heat transfer and the convective heat loss takes place from the convective zone. It can be seen from figure 5 that the temperatures of the lower part of the inclined cavity walls are relatively lower, while the temperatures of the upper parts of the walls are higher. The explanation behind this is that as air at ambient temperature is driven into the cavity receiver by the natural convective currents, the air adjacent to the receiver surface becomes hotter and lighter as it absorbs heat from the receiver surfaces and consequently flows up along the cavity wall. As a result of this, hot stagnant air appears only at the top of the cavity receiver. Eventually, the hot air leaves the cavity through the aperture and is then cooled by the ambient.

From Figure 6, it is observed that the convective heat loss varies non-linearly with receiver angle inclination at high operating temperatures. However, it is approximately linear at 400 K. The convective heat loss is at a minimum for all operating temperatures when the receiver aperture orientation is downwards. This supports the assumption of negligible convective heat loss with the receiver in this position as observed by other researchers. The maximum heat loss occurs when the receiver aperture is oriented at  $0^\circ$ . It is also observed that the effect of angle of inclination on convection heat loss is more significant for a higher receiver temperature. For example, the percentage decrease of the convection heat loss from  $0^\circ$  to  $90^\circ$  is about 68.87% for 1 000 K operating temperature in contrast to about 10% at 400 K. This can be attributed to the fact that the convection zone extends as the receiver moves anticlockwise thus causing an increase in convection heat loss.

The convection heat loss from the receiver was estimated for operating temperatures ranging from 400 K to 1 000 K at intervals of 200 K. From Figure 7, it was found that the convection heat loss increased tremendously with increasing receiver operating temperature. The effect of inclination angle on convection heat loss was not much at

lower operating temperatures compared with high operating temperatures where it was significantly higher. It is further observed from Figure 7 that the convection heat loss is closely linearly dependent on operating temperature.

#### **4.2 Effects of aperture size on natural convection heat loss**

To explore the effects of aperture size on natural convection heat loss, the diameter of aperture was varied from 60 mm to 120 mm at 800 K operating temperature. Figure 8 shows the variation of convection heat loss with the aperture size at different inclination angles.

It is clear from Figure 8 that as the aperture size becomes larger the convection heat loss also increases. However, the growth of the convection heat loss at 75° and 90° is minimal in comparison with the growth at other inclination angles. This is due to the fact that, as the cavity receiver moves anticlockwise, the convection zone expands apparently with increasing inclination angle, which definitely leads to considerable increment of the convection heat loss. This also explains that convection heat loss is not significantly affected when the receiver is near downwards-facing as confirmed by the curves for 75° and 90°. This leads to the conclusion that effect of aperture size on convection heat loss is actually closely related to the receiver inclination angle.

#### **4.3 The comparison of the Boussinesq and the non-Boussinesq fluid models**

For the fluids modelled as Boussinesq incompressible, the fluid properties were assumed constant and the density was treated as a linear function of temperature only and was assumed to be independent of pressure. Temperature-dependent air properties were used for the non-Boussinesq model to account for the air property variations. The comparison between the Boussinesq and the non-Boussinesq fluid models were made at equal equivalent Rayleigh number (Ra). Figure 9 and Figure 10 show the variation of the convection heat loss with inclination angles of the receiver for the Boussinesq and the non-Boussinesq fluid models. It can be seen from Figure 9 that at the receiver operating temperature of 400 K, the non-Boussinesq solution agreed with the Boussinesq solution with a maximum deviation of 6.1% when the receiver was at 0° inclination and a minimum of 1.7% at 90° inclination angle. Comparison of the non-Boussinesq and Boussinesq fluid models at 1 000 K operating temperature shows larger deviations with a maximum deviation of 19.48% at 0° inclination angle and a minimum deviation of 7.7% at 90° inclination angle as shown in Figure 10. It is therefore observed that the Boussinesq fluid model provides good approximation of air density data and other air properties only in the regime with a small temperature difference. An increase in the temperature difference leads to a growth in air properties error between the Boussinesq approximation and the non-Boussinesq fluid model. Without accurate predictions for the density and other air properties, the results



obtained based on the Boussinesq incompressible fluid model probably cannot reflect the real phenomenon taking place in the cavity receiver, therefore, the Boussinesq solution can be regarded as the solution for the limiting case with a small operating temperature difference.

#### **4 CONCLUSIONS**

A numerical investigation was conducted on a modified cavity receiver to quantify the natural convection heat loss and to determine the effects of the operating temperature, receiver inclination angle and aperture size on the heat loss. The effects of the variation of air properties were also accounted for by using polynomial relationships for density, specific heat capacity at constant pressure and dynamic viscosity.

It was observed that the convective heat loss varied non-linearly with receiver angle inclination at high operating temperatures. The convection heat loss was at a minimum for all operating temperatures when the receiver aperture orientation was facing downwards. The maximum heat loss occurred when the receiver aperture was oriented at  $0^\circ$ . It was found that the convective heat loss increased tremendously with increasing receiver operating temperature and the effect of inclination angle on convection heat loss was not much at lower operating temperatures compared with high operating temperatures where it was significantly higher.

It is clear that, as the aperture size became larger, the convection heat loss also increased. However, the growth of the convection heat loss at  $75^\circ$  and  $90^\circ$  was minimal in comparison with the growth at other inclination angles. This leads to the conclusion that the effect of aperture size on convection heat loss is actually closely related to the receiver inclination angle.

The comparison between the Boussinesq fluid and the non-Boussinesq fluid models showed some agreement at lower operating temperatures with a maximum deviation of 6.1%. However, the deviation was much higher at high operating temperatures with a maximum deviation of 19.48%.

## ACKNOWLEDGEMENT

The authors acknowledge the support of the Department of Mechanical and Aeronautical Engineering, University of Pretoria and the National Research Foundation.

## NOMENCLATURE

### *Abbreviation*

ANU            Australia National University

### Symbols

A            Area,  $m^2$   
D            Cavity diameter, m  
d            Aperture diameter, m  
C<sub>p</sub>          Specific heat capacity, J/(kg.K)  
H            Heat transfer coefficient, W/( $m^2K$ )

K            Kelvin  
k            Thermal conductivity, W/( $mK$ )  
kg          Kilogram  
m          Metre  
N          Newton's  
Nu         Nusselt number  
P          Pressure, Pa  
Pa         Pascal  
Q          Heat loss, W  
Ra         Raleigh number  
s          Seconds  
T          Temperature, K  
V          Velocity, m/s  
W          Watt  
X          Mass force vector, N/kg  
 $\varphi$          Receiver inclination angle, degree  
 $\rho$          Density of air,  $kg/m^3$   
 $\mu$          Dynamic viscosity,  $kg/(m.s)$

### *Subscript*

c            convection  
s            surface  
 $\infty$          ambient  
h            hold  
exp         experimental  
num         numerical  
anal         analytical

## REFERENCE

1. LeQuere, P., Penot, E. and M. Mirenayot. (1981). Experimental study of heat loss through natural convection from an isothermal cubic open cavity.
2. Harris, J.A. and T.G. Lenz. (1985). Thermal performance of solar concentrator/cavity receiver systems. *J Solar Energy* 34(2):135-142.
3. Clausing, A.M. (1983). Convective losses from cavity solar receivers - comparisons between analytical predictions and experimental results. *J Solar Energy Engineering* 105:29-33.
4. Siangsukone, P. and K. Lovegrove. (2002). Modelling of a steam based paraboloidal dish concentrator using the computer source code TRNSYS. *Proceedings of Solar - Australian and New Zealand Solar Energy Society Paper 1*.
5. Taumoefolau, T. and K. Lovegrove. (2002). An experimental study of natural convection heat loss from a solar concentrator cavity receiver at varying orientation. *Proceedings of Solar - Australian and New Zealand Solar Energy Society Paper 1*.
6. Sendhil Kumar, N. and K.S. Reddy. (2007). Numerical investigation of natural convection heat loss in modified cavity receiver for fuzzy focal solar dish concentrator. *J Solar Energy* 81:846-855.
7. Sendhil Kumar, N. and K.S. Reddy. (2008). Comparison of receivers for solar dish collector system. *Energy Conversion and Management* 49:812-819.
8. Reddy, K.S. and N. Sendhil Kumar. (2008). Combined laminar natural convection and surface radiation heat transfer in a modified cavity receiver of solar parabolic dish. *J Thermal Sciences* 47:1647-1657.
9. Reddy, K.S. and N. Sendhil Kumar. (2009). An improved model for natural convection heat loss from modified cavity receiver of solar dish concentrator. *J Solar Energy* 83:1884-1892.
10. Prakash, M., Kedare, S.B. and J.K. Nayak. (2009). Investigations on heat losses from a solar cavity receiver. *J Solar Energy* 83:157-170.
11. Wu, S., Xiao, L. and Y. Li. (2011). Effect of aperture position and size on natural convection heat loss of a solar heat-pipe receiver. *J Applied Thermal Engineering* 31:2787-2796.
12. Zografos, A.I., Martin, W.A. and J.E. Sunderland. (1987). Equations of properties as a function of temperature for seven fluids. *J Computer Methods in Applied Mechanics and Engineering* 61:177-187.
13. Khubeiz, J.M., Radziemska, E., Lewandowski, W.M. (2002). Natural convective heat transfers from an isothermal horizontal hemispherical cavity. *J of Applied Energy* 73:261-275.

## **Figure Legends**

**Figure 1.** Schematic of a parabolic dish concentrating collector with modified cavity model

**Figure 2.** Typical computational grid for the numerical analysis of the modified cavity receiver

**Figure 3.** Numerical model and boundary conditions of the modified cavity receiver

**Figure 4.** Temperature contours of mid plane of upward open hemispherical cavity

**Figure 5.** Temperature contours of the cavity at 400 K for various inclination angles

**Figure 6.** Variation of convection heat loss with inclination angle

**Figure 7.** Variation of convection heat loss with operating temperature

**Figure 8.** Variation of convection heat loss with aperture diameter at 800 K

**Figure 9.** Variation of convection heat loss with inclination angle at 400 K

**Figure 10.** Variation of convection heat loss with inclination angle at 1 000 K

**Figure 1** Schematic of a parabolic dish concentrating collector with modified cavity model

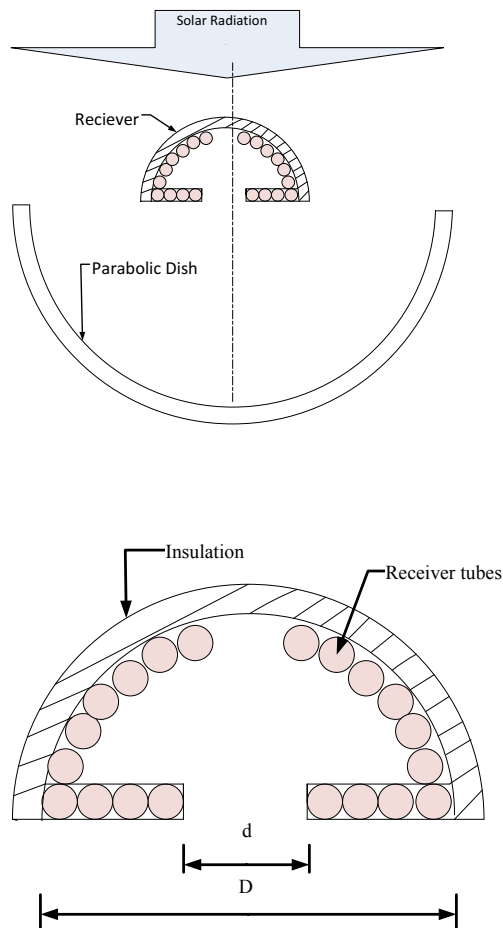


**Figure 2** Typical computational grid for the numerical analysis of the modified cavity receiver

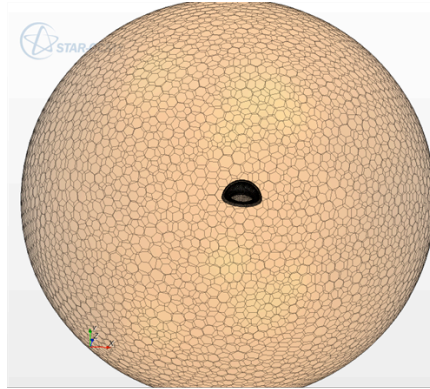


**Figure 3** Numerical model and boundary conditions of the modified cavity receiver

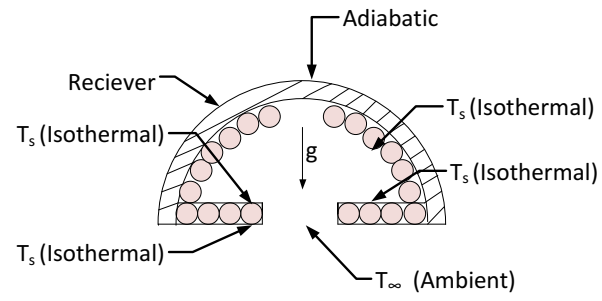


**Figure 4** Temperature contours of mid plane of upward open hemispherical cavity

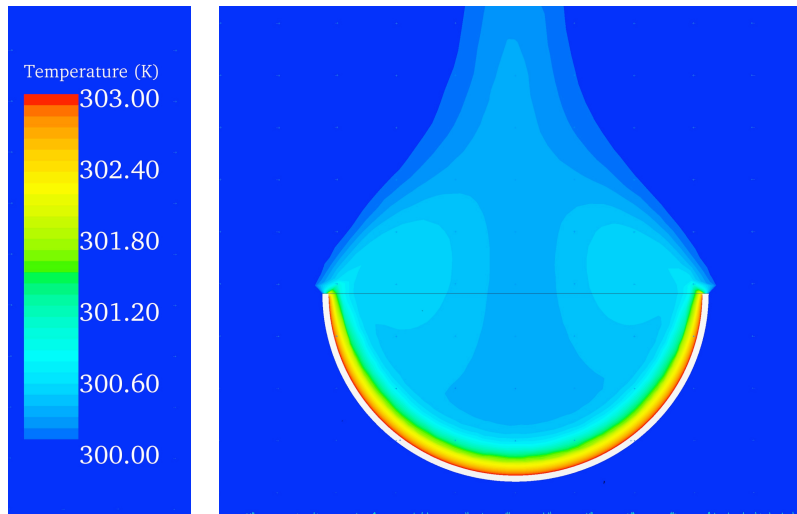




**Figure 5** Temperature contours of the cavity at 400 K for various inclination angles

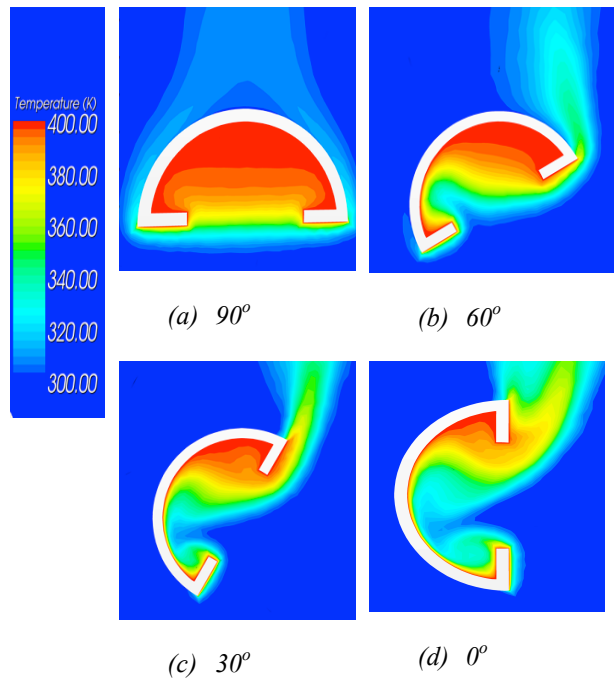


**Figure 6** Variation of convection heat loss with inclination angle

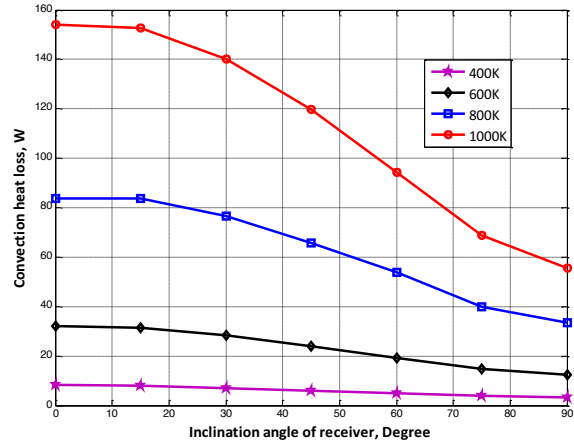


**Figure 7** Variation of convection heat loss with operating temperature

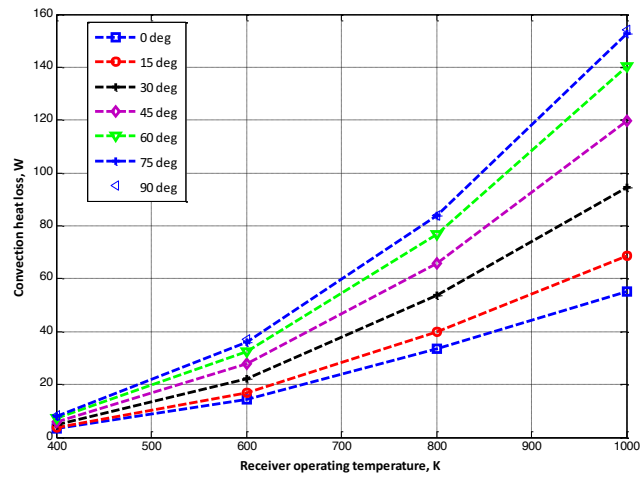
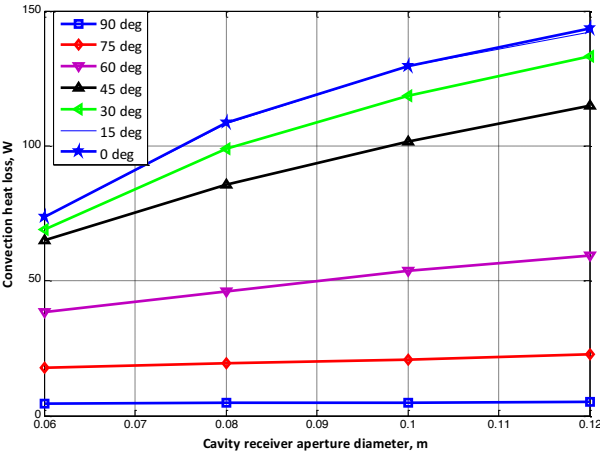
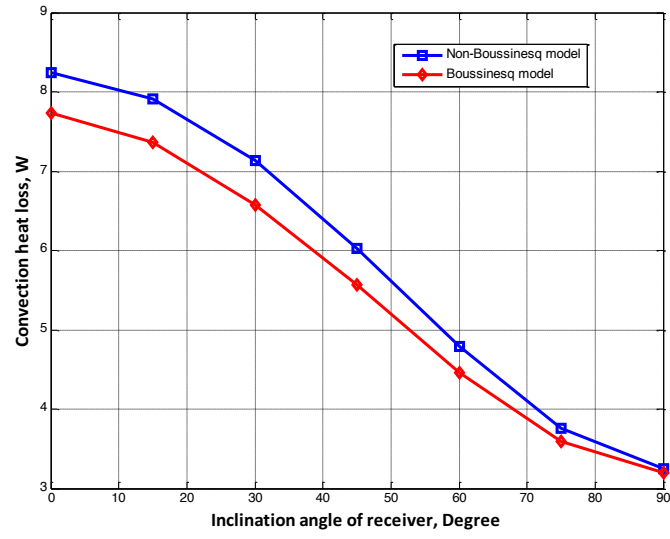


Figure 8 Variation of convection heat loss with aperture diameter at 800 K



**Figure 9** Variation of convection heat loss with inclination angle at 400 K



**Figure 10** Variation of convection heat loss with inclination angle at 1 000 K

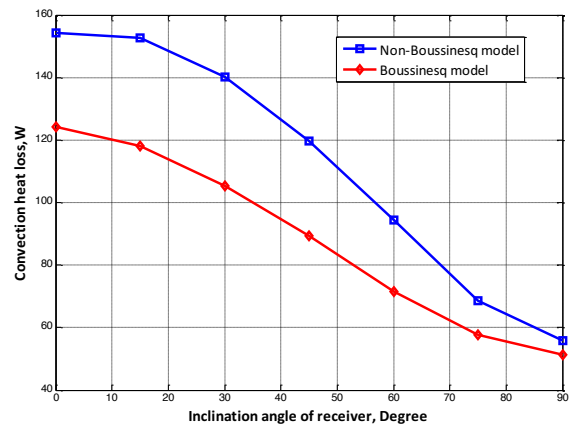


Table 1 Average Nusselt numbers for different grids

Number Of cells	Nusselt number	Relative Deviation
$1.85 \times 10^5$	12.3475	
$1.70 \times 10^5$	12.3463	0.000101
$1.58 \times 10^5$	12.2686	0.006288
$1.43 \times 10^5$	12.3802	-0.00909
$1.38 \times 10^5$	12.3123	0.005486

**Table 2** Validation of the present numerical procedure using experimental convective Nusselt number

Rayleigh number	Nusselt number from Khubeiz et al. (2002)			Nusselt number from present numerical procedure	Percentage of deviation from experimental value
	Nu <sub>exp</sub>	Nu <sub>num</sub>	Nu <sub>anal</sub>		
$2.4864 \times 10^6$	12.55	13.50	11.75	11.74	6.45
$1.1511 \times 10^7$	18.41	19.80	17.24	18.82	-2.23